International Journal of Heat and Mass Transfer 52 (2009) 5784–5791

Contents lists available at ScienceDirect

International Journal of Heat and Mass Transfer

journal homepage: www.elsevier.com/locate/ijhmt

Critical times in multilayer diffusion. Part 2: Approximate solutions

R.I. Hickson [a], S.I. Barry [a,b,*], G.N. Mercer [b]

[a] School of Physical, Environmental and Mathematical Sciences, University of New South Wales at ADFA, Northcott Drive, Canberra, ACT 2600, Australia
[b] National Centre for Epidemiology and Public Health, Australian National University, Canberra, ACT 0200, Australia

ARTICLE INFO

Article history:
Received 1 April 2009
Received in revised form 17 August 2009
Available online 18 September 2009

Keywords:
Diffusion
Multilayer
Critical time
Time lag
Laminates
Composite materials

ABSTRACT

Traditional averaging methods for multilayer diffusion give inaccurate approximations of critical time behaviour, such as the heating time of a material. In particular, they fail to capture the importance of layer order. We use a perturbation expansion of an exact solution to find a simple approximate solution which accurately describes the critical time for transport across multiple layers. This approximate solution is then used to find a correction for the averaging method which captures the key critical time behaviour.

1. Introduction

Critical times through multilayered mediums are important for a number of applications, from annealing steel coils [1–3] to determining the effectiveness of drug carriers inserted into living tissue [4]. For example, in heat transport the critical diffusion time, or mean action time [5–7], is the time taken for a material to reach a defined temperature after a temperature change is imposed on the boundaries. A review of applications, analytic solutions, and critical time definitions is included in the companion paper, Hickson et al. [8], hereafter referred to as "Part 1 [8]". This companion paper gives exact solutions for linear diffusion through multiple layers and numerically explores the behaviour of the critical time as a function of the number of layers. Other previous work [9] also explores a critical time, although for a simpler case with a different definition. In this second part, we analyse the analytic solutions of Part 1 [8] to find simple approximate expressions for the diffusion and the critical time. For completeness the main results of the companion paper are reproduced here with minimal explanation. Due to the complexity of the perturbation method only a specific set of boundary and interface conditions are used, rather than the more general conditions applied in Part 1 [8]. A solution for the more general conditions is non-trivial and the subject of further research.

The standard diffusion equation is applicable in each layer:

$$\frac{\partial U_i}{\partial t} = D_i \frac{\partial^2 U_i}{\partial x^2}, \quad i \in [1, n], \tag{1}$$

where $U_i(x,t)$ is the temperature in layer i at position x for $x_{i-1} < x < x_i$ and time t, as depicted in Fig. 1. The boundary conditions used here assume an imposed 'temperature':

$$U_1(x_0, t) = \theta_1, \quad U_n(x_n, t) = \theta_2, \tag{2}$$

where θ_1 and θ_2 are constants. In a heat diffusion context this represents external temperatures being forced on the medium, for example in the case of the steel coil being annealed [1–3]. Matching conditions are assumed for the interfaces where

$$U_i(x_i, t) = U_{i+1}(x_i, t), \tag{3}$$

$$\kappa_i \frac{\partial U_i}{\partial x}\bigg|_{x_i} = \kappa_{i+1} \frac{\partial U_{i+1}}{\partial x}\bigg|_{x_i}, \tag{4}$$

and $i = 1, 2, \ldots, n-1$ where $\kappa_i = \rho_i c_i D_i$ is layer conductivity, ρ_i is layer density, c_i is layer specific heat, and an 'interface' is the common boundary between two layers. Eqs. (3) and (4) represent continuity in temperature and flux respectively. For simplicity, we assume $\rho_i c_i = 1$.

As discussed in Part 1 [8], a standard critical time approximation is

$$t_{\text{av}} = \frac{L^2}{6 D_{\text{av}}}, \tag{5}$$

where D_{av} is the series averaged diffusivity for layered materials, given by

* Corresponding author. Address: National Centre for Epidemiology and Public Health, Australian National University, Canberra, ACT 0200, Australia. Tel.: +61 02 6125 9506; fax: +61 02 6125 0740.
E-mail addresses: R.I.Hickson@gmail.com (R.I. Hickson), Steven.Barry@anu.edu.au (S.I. Barry).

0017-9310/$ - see front matter © 2009 Elsevier Ltd. All rights reserved.
doi:10.1016/j.ijheatmasstransfer.2009.08.012

Nomenclature

c_i	layer specific heat
$D = d^2$	single layer diffusivity
$D_{\text{av}} = d_{\text{av}}^2$	average diffusivity
$D_{\text{eff}} = d_{\text{eff}}^2$	effective diffusivity
$D_i = d_i^2$	layer diffusivity
$f(x)$	initial condition
L	total length of medium
l_i	layer width
n	total number of layers
t	time
t_{av}	typical critical time
t_c	multilayer critical time
t_s	single layer critical time
$U(x,t)$	temperature
$v(x,t)$	transient solution
x	spatial position
$w(x)$	steady state solution

Additional notation

$[A,B]$	shorthand for $n/2$ biperiodic layers, material properties D_A, D_B as $ABAB\ldots AB$

Greek symbols

α	proportion of the steady state
κ_i	layer conductivity
λ_m	multilayer eigenvalues
μ_m	single layer eigenvalues
ρ_i	layer density
θ_1	boundary condition at $x = x_0$
θ_2	boundary condition at $x = x_n$

Subscripts

i	layer index
m	eigenvalue index

$$\frac{L}{D_{\text{av}}} = \sum_{i=1}^{n} \frac{l_i}{D_i}, \tag{6}$$

where L is the total medium length, l_i is the width of layer i, and D_i is the diffusivity of layer i. The definition used in this paper was described in Part 1 [8], where the value of $t = t_c$ is defined such that

$$\int_{x=0}^{L} U(x,t_c)\,dx = \alpha \int_{x=0}^{L} w(x)\,dx, \tag{7}$$

where $U(x,t)$ is the temperature, $0 < \alpha < 1$ is a chosen constant, and $w(x)$ is the steady state.

In Part 1 [8] we demonstrated that the standard approximations given by Eqs. (5) and (6) give inaccurate results and the numerical simulations illustrate a complex critical time behaviour. In this article we will find general approximate solutions which improve on these results. For example, for a medium with $\theta_1 = 1,\ \theta_2 = 0$, and initial condition $f(x) = 0$, with n layers $ABAB\ldots AB$, denoted as $[A,B]$, the critical time is

$$t_c \approx \frac{L^2}{6D_{\text{av}}} - \left(1 - \frac{D_{\text{av}}}{D_A}\right)\frac{Ll}{\pi^2 D_{\text{av}}}, \tag{8}$$

(taken from Section 6, Eq. (53)). A more general version of this is Eq. (43) in Section 4. The expression for critical time is then used to find a correction for Eq. (6).

In the next section we will outline the key results of the analytic solution found in Part 1 [8] for the simpler boundary conditions considered here. In Section 3 a general perturbation solution is derived using results detailed in Appendix A. In Section 4 this complicated perturbation solution is used to derive the general results equivalent to Eq. (8) above. These solutions are analysed in Section 5 and examples discussed in Section 6.

2. Exact solutions

The exact solutions were found using separation of variables, outlined in Part 1 [8], and for completeness the key equations are given here. We only consider the simpler case of constant boundary conditions, hence in the notation of Part 1 [8], $a_1 = 1 = a_2$ and $b_1 = 0 = b_2$.

When the initial condition $f(x) = 0$, the single layer solution is

$$U(x,t) = \theta_1 + \frac{(\theta_2 - \theta_1)x}{L} + 2\sum_{m=1}^{\infty} \frac{\left(\theta_2(-1)^m - \theta_1\right)}{m\pi} e^{-\mu_m^2 t} \times \sin\left(\frac{m\pi x}{L}\right), \tag{9}$$

where μ_m are the eigenvalues,

$$\mu_m = \frac{m\pi d}{L}, \quad m = 1,2,3,\ldots, \tag{10}$$

and we use the simpler notation $d = \sqrt{D}$. Using Eq. (7) the critical time for a single layer is then given by

$$t_s \approx \frac{L^2}{\pi^2 D} \log\left\{\frac{8}{\pi^2(1-\alpha)}\right\} \tag{11}$$

for the leading eigenvalue. The critical time must be positive, therefore $(1 - 8/\pi^2) < \alpha < 1$. Equating this to Eq. (5) gives $\alpha = 1 - (8/\pi^2)\exp(-\pi^2/6) \approx 0.8435$.

The exact solution for multilayers is

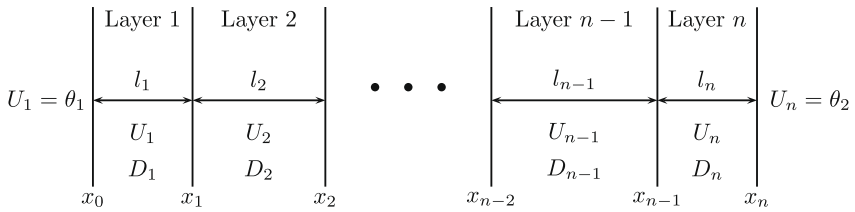

Fig. 1. Multilayer schematic with boundary conditions where θ_1 and θ_2 are constants. Here U_i is the temperature in layer i at time t, D_i is the diffusivity of a given layer and l_i is the width of the layer.

$$U_i(x,t) = w_i(x) + \sum_{m=1}^{\infty} C_m e^{-\lambda_m^2 t} X_{i,m}(x), \tag{12}$$

where the summation constant is given by

$$C_m = \frac{\sum_{i=1}^{n} \int_{x_{i-1}}^{x_i} g_i(x) X_{i,m}(x)\,dx}{\sum_{i=1}^{n} \int_{x_{i-1}}^{x_i} X_{i,m}^2(x)\,dx}, \tag{13}$$

here $g_i(x) = f_i(x) - w_i(x)$, the eigenvalues, λ_m, are defined by the transcendental expression

$$J_{n,m} \sin\left(\lambda_m \frac{l_n}{d_n}\right) + K_{n,m} \cos\left(\lambda_m \frac{l_n}{d_n}\right) = 0, \tag{14}$$

and the eigenfunctions are

$$X_{i,m}(x) = J_{i,m} \sin\left(\frac{\lambda_m}{d_i}(x - x_{i-1})\right) + K_{i,m} \cos\left(\frac{\lambda_m}{d_i}(x - x_{i-1})\right). \tag{15}$$

The coefficients of the eigenfunctions are recursively defined:

$$J_{i+1,m} = \frac{d_i}{d_{i+1}}\left[J_{i,m} \cos\left(\lambda_m \frac{l_i}{d_i}\right) - K_{i,m} \sin\left(\lambda_m \frac{l_i}{d_i}\right)\right], \tag{16}$$

$$K_{i+1,m} = J_{i,m} \sin\left(\lambda_m \frac{l_i}{d_i}\right) + K_{i,m} \cos\left(\lambda_m \frac{l_i}{d_i}\right), \tag{17}$$

where $J_{1,m} = 1$ and $K_{1,m} = 0$. The steady state solution is

$$w_i(x) = q_i(x - x_{i-1}) + h_i, \tag{18}$$

where $h_1 = \theta_1$,

$$q_i = \frac{D_{\text{av}}(\theta_2 - \theta_1)}{LD_i}, \tag{19}$$

$$h_i = \theta_1 + \frac{D_{\text{av}}(\theta_2 - \theta_1)}{L} \sum_{j=1}^{i-1} \frac{l_j}{D_j}. \tag{20}$$

The critical time for multiple layers, t_c, is found by solving

$$(1-\alpha) \sum_{i=1}^{n} \int_{x_{i-1}}^{x_i} w_i(x)\,dx + \sum_{i=1}^{n} \int_{x_{i-1}}^{x_i} v_i(x, t_c)\,dx = 0. \tag{21}$$

Substituting Eq. (12) into this gives

$$(1-\alpha) \sum_{i=1}^{n} \left\{h_i l_i + \frac{q_i l_i^2}{2}\right\} + \sum_{i=1}^{n} d_i \sum_{m=1}^{\infty} \frac{C_m}{\lambda_m} e^{-\lambda_m^2 t_c} \Psi_{i,m} = 0, \tag{22}$$

where

$$\Psi_{i,m} = J_{i,m}\left\{1 - \cos\left(\frac{\lambda_m l_i}{d_i}\right)\right\} + K_{i,m} \sin\left(\frac{\lambda_m l_i}{d_i}\right). \tag{23}$$

The numerical results shown in Part 1 [8] provided some insight as to how the critical time behaviour differs for multiple layers as opposed to a single medium, however it fails to explain why this difference occurs. Hence in the next section we will explore an approximate perturbation of the exact solution which will illuminate the causes for this behaviour.

3. Perturbation

In this section we perform a perturbation analysis on the exact solution, Eq. (12), to find simple approximate solutions which represent the behaviour shown in the results of Part 1 [8]. A number of assumptions are made in the process. First, a biperiodic region, $[A,B]$, is used. Second, the total length of the medium, L, is fixed and the widths of the 'A' and 'B' layers are assumed to be equal, hence $l_A = l_B = l = L/n$.

Example biperiodic temperature profiles are shown in Fig. 2 for $L = 1,\ \theta_1 = 1,\ \theta_2 = 0,\ n = 10,\ l = 0.1,\ D_A = 1,$ and $D_B = 0.1,$ at times $t = 0.01,\ 0.2, 1$.

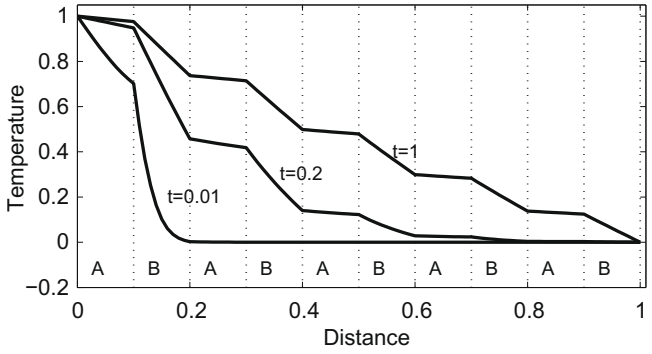

Fig. 2. Temperature profile for a biperiodic region [1,0.1], with $n = 10,\ \theta_1 = 1,\ \theta_2 = 0,\ l = 0.1$, at times $t = 0.01, 0.2, 1$.

Biperiodic layers have been studied before, such as the previously mentioned work on steel coils [1] which consists of biperiodic layers of steel and air, and the analytic and numerical work of Azeez and Vakakis [10], Ash et al. [11,12], and Barrer [13].

The perturbation parameter chosen is $l = L/n$, which is small for large n. Hence as $n \to \infty,\ l \to 0$. A complication arises since $nl = L$, which is of order one. Hence any terms including il, where i is the layer number, are of indeterminate order and must be treated with care.

The solutions in the 'A' and 'B' layers are sufficiently different (see Fig. 2) that they must be considered separately. Hence there will be two perturbation series, one for U_{i_A} and another for U_{i_B}.

Due to the complexity of the problem, each of the variables in Eq. (12) are treated separately. That is, the steady state, $w_i(x)$, is considered in Section 3.1, the eigenfunction, $X_{i,m}(x)$, in Section 3.2, the eigenvalues, λ_m, in Section 3.3, and finally the summation coefficient, C_m, in Section 3.4. The complete solution is constructed in Section 3.5. Due to the algebra being both long and detailed, the computer algebra system Maple [14] was used to calculate and check the work done in Sections 3.1–3.5, including Appendix A.

3.1. Steady state

The steady state solution for multilayer diffusion, detailed in Eqs. (18)–(20), are now calculated in terms of the biperiodic assumptions outlined earlier in Section 3.

The summation term in Eq. (20) is of particular importance in simplifying the steady state, and requires considering whether layer i is material 'A' or material 'B' in the $[A,B]$ structure. If i corresponds to an 'A' layer then $(i-1)$ corresponds to a 'B' layer, so

$$\sum_{j=1}^{i-1} \frac{1}{D_j} = \frac{i-1}{2}\left(\frac{1}{D_A} + \frac{1}{D_B}\right). \tag{24}$$

Eq. (6) can be rearranged for the $[A,B]$ structure with equal layer widths to show

$$\frac{1}{2}\left(\frac{1}{D_A} + \frac{1}{D_B}\right) = \frac{1}{D_{\text{av}}}. \tag{25}$$

Therefore,

$$\sum_{j=1}^{i-1} \frac{1}{D_j} = \frac{i-1}{D_{\text{av}}}, \tag{26}$$

which is expected since this summation is simply $(i-1)/2$ complete AB pairs. Similarly, if i corresponds to a 'B' layer then $(i-1)$ corresponds to an 'A' layer, so

$$\sum_{j=1}^{i-1}\frac{1}{D_j}=\frac{i}{D_{\rm av}}-\frac{1}{D_B}\equiv\frac{i-1}{D_{\rm av}}+\frac{1}{D_A}. \tag{27}$$

Therefore the constant h_i is rewritten as

$$h_{i_A}=\theta_1+\frac{(\theta_2-\theta_1)}{L}(i-1)\,l$$
$$h_{i_B}=\theta_1+\frac{(\theta_2-\theta_1)}{L}\left(i-\frac{D_{\rm av}}{D_B}\right)l, \tag{28}$$

where h_{i_A} is the constant in 'A' layers and h_{i_B} is the constant in 'B' layers.

By definition of the structure depicted in Fig. 1 and with the assumption that all widths are equal, then $i=x_i/l$ and $x_{i-1}=x_i-l$. Using these, the biperiodic structure, and substituting Eq. (28) into Eq. (18), gives

$$w_{i_A}=\theta_1+\frac{(\theta_2-\theta_1)x}{L}+\left(1-\frac{D_{\rm av}}{D_A}\right)\frac{(\theta_2-\theta_1)(x-x_{i-1}-l)}{L}, \tag{29}$$

$$w_{i_B}=\theta_1+\frac{(\theta_2-\theta_1)x}{L}-\left(1-\frac{D_{\rm av}}{D_A}\right)\frac{(\theta_2-\theta_1)(x-x_{i-1})}{L}, \tag{30}$$

where w_{i_A} is the steady state solution in 'A' layers, and w_{i_B} is the steady state solution in 'B' layers.

When $l\to 0$, $x_i\approx x_{i-1}\approx x$ so Eqs. (29) and (30) approach the single layer steady state solution, given by the first two terms in Eq. (9).

3.2. Eigenfunction, $X_{i,m}(x)$

Calculation of a perturbation series for the eigenfunctions, Eq. (15) is complicated by the recursive coefficients $J_{i,m}$ and $K_{i,m}$, Eqs. (16) and (17). Finding these coefficients as a perturbation series is non-trivial. To aid readability, this calculation is shown separately in Appendix A, with the final results given in Eqs. (68) and (69).

Substituting Eq. (68) into the eigenfunctions, Eq. (15), and using Maple to simplify the resulting perturbation series, gives the eigenfunctions when i corresponds to an A layer as

$$\begin{aligned}X_{i_A,m}(x)=\frac{1}{2}\Bigg\{&\left(1+\frac{d_A}{d_{\rm av}}\right)\sin\left(\omega_m(x_A+x_{i-1})\right)\\&+\left(1-\frac{d_A}{d_{\rm av}}\right)\sin\left(\omega_m(x_A-x_{i-1})\right)\Bigg\}+\frac{\omega_m}{4}\left(1-\frac{D_{\rm av}}{D_A}\right)\\&\times\left\{\cos(\omega_m(x_A-x_{i-1}))-\cos(\omega_m(x_A+x_{i-1}))\right\}l+O(l^2),\end{aligned} \tag{31}$$

with

$$x_A=\frac{(x-x_{i-1})d_{\rm av}}{d_A},\quad \omega_m=\frac{m\pi}{L}. \tag{32}$$

Similarly, using Eq. (69) gives

$$\begin{aligned}X_{i_B,m}(x)=\frac{d_A}{2}\Bigg\{&\left(\frac{1}{d_B}+\frac{1}{d_{\rm av}}\right)\sin(\omega_m(x_B+x_{i-1}))+\left(\frac{1}{d_B}-\frac{1}{d_{\rm av}}\right)\\&\times\sin(\omega_m(x_B-x_{i-1}))\Bigg\}+\frac{\omega_m}{4d_{\rm av}}\left(\frac{D_{\rm av}}{D_A}-1\right)\\&\times\left\{(2d_A+d^\star)\cos(\omega_m(x_B+x_{i-1}))+(2d_A-d^\star)\right.\\&\left.\times\cos(\omega_m(x_B-x_{i-1}))\right\}l+O(l^2)\end{aligned} \tag{33}$$

with

$$x_B=\frac{d^\star(x-x_{i-1})}{d_A},\quad d^\star=\sqrt{2D_A-D_{\rm av}}. \tag{34}$$

Note that $d=\sqrt{D}$ for subscripts A, B, and av. Although these expression can be rewritten using standard trigonometric identities, the resulting expressions yield no new insight.

When $l\to 0, x_i\approx x_{i-1}\approx x$ so

$$X_{i,m}(x)\to\frac{d_A}{d_{\rm av}}\sin\left(\frac{m\pi x}{L}\right) \tag{35}$$

for both the 'A' and 'B' cases. For a single layer, $d_A=d_{\rm av}=d_B$, hence reducing $X_{i,m}$ to the single layer eigenfunction in Eq. (9).

3.3. The eigenvalues

The eigenvalues, λ_m, satisfy Eq. (14). The constants $J_{n,m}$ and $K_{n,m}$ are a critical part of this equation and are found the same way as Eq. (69) in Appendix A, but by substituting $i=L/(2l)-1$, giving

$$\begin{aligned}J_{n,m}&=\frac{\sqrt{2D_A-D_{\rm av}}}{d_{\rm av}}\left[\cos\left(\frac{\lambda_m L}{d_{\rm av}}\right)+\frac{\lambda_m(D_A-D_{\rm av})}{2D_A d_{\rm av}}\sin\left(\frac{\lambda_m L}{d_{\rm av}}\right)l\right]+O(l^2)\\ \times K_{n,m}&=\frac{d_A}{d_{\rm av}}\sin\left(\frac{\lambda_m L}{d_{\rm av}}\right)-\frac{\lambda_m(D_A-D_{\rm av})}{d_A D_{\rm av}}\cos\left(\frac{\lambda_m L}{d_{\rm av}}\right)l+O(l^2).\end{aligned} \tag{36}$$

These are substituted into Eq. (14) which is then expanded as a perturbation series in l to give

$$\lambda_m=\frac{m\pi d_{\rm av}}{L}-\left(1-\frac{D_{\rm av}}{D_A}\right)^2\frac{m^3\pi^3 d_{\rm av}}{24L^3}\,l^2+O(l^4). \tag{37}$$

Note the zeroth order is equivalent to the single layer eigenvalue, Eq. (10).

3.4. Summation coefficient, C_m

If the initial condition $f_i(x)=0$, the summation coefficient, Eq. (13), is given by

$$C_m=\frac{\sum_{i=1}^{n}\int_{x_{i-1}}^{x_i}-w_i(x)X_{i,m}(x)\,dx}{\sum_{i=1}^{n}\int_{x_{i-1}}^{x_i}X_{i,m}^2(x)\,dx}. \tag{38}$$

Since w_i and $X_{i,m}$ are split into 'A' and 'B' layer solutions, this becomes

$$C_m=\frac{\sum_{i\equiv A}^{n-1}\int_{x_{i-1}}^{x_i}-w_{i_A}(x)X_{i_A,m}(x)\,dx+\sum_{i\equiv B}^{n}\int_{x_{i-1}}^{x_i}-w_{i_B}(x)X_{i_B,m}(x)\,dx}{\sum_{i\equiv A}^{n-1}\int_{x_{i-1}}^{x_i}X_{i_A,m}^2(x)\,dx+\sum_{i\equiv B}^{n}\int_{x_{i-1}}^{x_i}X_{i_B,m}^2(x)\,dx}, \tag{39}$$

where $i\equiv A$ denotes 'A' layers and $i\equiv B$ denotes 'B' layers. Each of the four integrals were evaluated separately and a perturbation series calculated for each. The resulting coefficient has the form

$$C_m=C_m^{(0)}+C_m^{(1)}\,l+C_m^{(2)}\,l^2+\ldots, \tag{40}$$

where

$$C_m^{(0)}=\frac{2d_{\rm av}[\theta_2(-1)^m-\theta_1]}{m\pi d_A}. \tag{41}$$

Surprisingly all higher order terms calculated were zero ($C_m^{(1)}$, etc.), although investigation of this is the subject of further research. For a single layer, $d_A=d_{\rm av}=d_B$, hence this is equivalent to the summation constant in Eq. (9).

3.5. Construction of complete solution

The complete solution is constructed by substituting the results from Sections 3.1–3.4 into Eq. (12). A further perturbation series of this and simplifications give

$$U_A(x,t)=U_A^{(0)}(x,t)+U_A^{(1)}(x,t)\,l+O(l^2)\quad\text{and}$$
$$U_B(x,t)=U_B^{(0)}(x,t)+U_B^{(1)}(x,t)\,l+O(l^2). \tag{42}$$

For readability these terms are only explicitly shown in Appendix B, Eqs. (70)–(74).

When $l \to 0$, $x_i \approx x_{i-1} \approx x$ so $U_A(x,t) \to U(x,t)$ and $U_B(x,t) \to U(x,t)$, Eq. (9). This behaviour is expected since it has been shown [8,9] the averaging of material properties works as the number of layers approaches infinity, which is equivalent to $l \to 0$.

4. Critical time

The perturbed average critical time is calculated by substituting Eq. (42) into Eq. (21). The resulting perturbation series has the form

$$t_c = t_c^{(0)} + t_c^{(1)} l + t_c^{(2)} l^2 + t_c^{(3)} l^3 + O(l^4), \tag{43}$$

where

$$t_c^{(0)} = \frac{L^2}{\pi^2 D_{\text{av}}} \log\left\{\frac{8}{\pi^2(1-\alpha)}\right\}, \tag{44}$$

$$t_c^{(1)} = \frac{L}{\pi^2 D_{\text{av}}}\left(1 - \frac{D_{\text{av}}}{D_A}\right)\Theta, \tag{45}$$

$$t_c^{(2)} = -\frac{L^0}{\pi^2 D_{\text{av}}}\left(1 - \frac{D_{\text{av}}}{D_A}\right)^2\left[\frac{\pi^2}{12}\log\left\{\frac{8}{\pi^2(1-\alpha)}\right\} + \frac{\Theta^2}{2} + \frac{\pi^2}{24}\right], \tag{46}$$

$$t_c^{(3)} = \frac{L^{-1}}{\pi^2 D_{\text{av}}}\left(1 - \frac{D_{\text{av}}}{D_A}\right)^3\left[\frac{\pi^2\Theta}{12} + \frac{\Theta^3}{3}\right], \tag{47}$$

$\Theta = (\theta_2 - \theta_1)/(\theta_2 + \theta_1)$, and $t_c^{(0)} \equiv t_s$, Eq. (11). We note that although there do appear to be patterns within these results, for example the ordered powers of L, Θ^n/n and $\left(1 - \frac{D_{\text{av}}}{D_A}\right)$, we were unable to find a general expression for the nth order term. Calculation of higher order terms is non-trivial with the apparent simplicity of the final results belying the limitations in Maple computational ability.

4.1. Effective diffusivity

Another interpretation of the critical time is to assume it is given by the standard diffusive time for a single layer, Eq. (11), with $D = D_{\text{eff}}$:

$$t_c \approx \frac{L^2}{\pi^2 D_{\text{eff}}} \log\left\{\frac{8}{\pi^2(1-\alpha)}\right\}, \tag{48}$$

but where D_{eff} is correctly defined for a multilayered material. Setting Eq. (48) equal to Eq. (43) and rearranging for D_{eff} gives

$$D_{\text{eff}} = D_{\text{av}} - \left(1 - \frac{D_{\text{av}}}{D_A}\right)\frac{(\theta_2 - \theta_1)D_{\text{av}}}{L(\theta_1 + \theta_2)\log\left\{\frac{8}{\pi^2(1-\alpha)}\right\}}\, l + O(l^2). \tag{49}$$

Note the zeroth order term is the average diffusivity, D_{av}.

5. Results

To illustrate the perturbation results the critical time is calculated as a function of the number of repeated layers, $n/2$, using the assumptions outlined in Section 3. That is, a biperiodic region is used, represented by the notation $[D_A, D_B]$, with equal widths for all layers. The diffusivity values of [1,0.1] and [0.1,1] are used. The region is defined with $x_0 = 0$ to $x_n = 1$, hence $L = 1$. The initial condition used is $f_i(x) = 0$. The boundary conditions are set to $\theta_1 = 1$ and $\theta_2 = 0$. To allow comparison with the other results from the literature [11–13], detailed in Appendix C, we choose the standard value of $\alpha = 0.8435$ as determined in Section 2.

Results in Fig. 3 indicate the critical time calculated numerically from the exact solution, Eq. (22) for both [1,0.1] and [0.1,1] scenarios. The solution using the traditional averaged diffusivity, $D_{\text{av}} = 0.18$, approximated from Eqs. (5) and (6) are also shown.

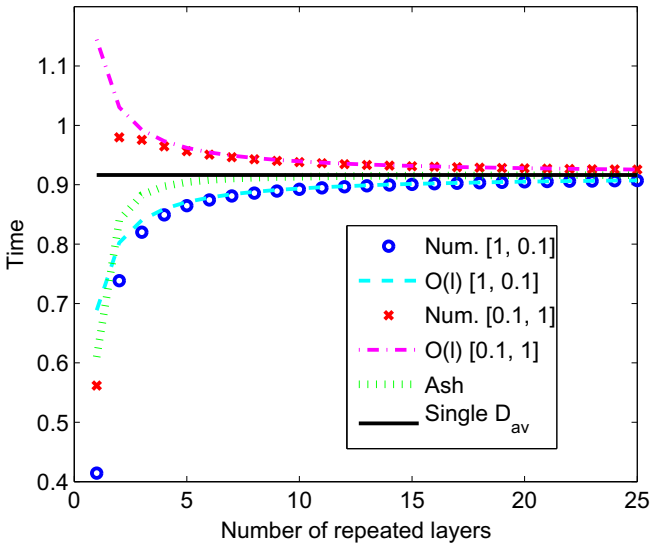

Fig. 3. Critical time versus number of repeated layers for a biperiodic region. Here $L = 1$, $l_i = 1/n$, diffusivities are $[D_A, D_B] = [1, 0.1]$ or $[0.1, 1]$, and $\alpha = 0.8435$. 'Num.' solutions correspond to the numerically found critical time, Eq. (22), 'O(l)' refers to the first order perturbation approximation, Eq. (43), 'Ash' refers to Eq. (76), and 'Single Dav' refers to the single layer critical time, Eq. (11), with $D_{\text{av}} = 0.18$ using Eq. (6).

Additionally the first order approximations from Eq. (43), for both [1,0.1] and [0.1,1] scenarios, and the solution from Ash et al. [11], Eq. (76), are shown. The results from Fig. 3 illustrate the accuracy of just the first order perturbation approximation, along with the relative inaccuracy of the series-averaged approximation D_{av}, and the results from earlier literature [11]. The first order solution does not replicate the behaviour of the numerically found exact solution for 1 and 2 repeated layers (that is *AB* and *ABAB* layers). This is to be expected since for 2 repeated layers the perturbation parameter is $l = 0.25$, which is relatively large. As the number of layers increases, all solutions converge to the single layer solution with the averaged diffusivity, D_{av} as expected.

To illustrate the second order solutions, Fig. 4 depicts the numerically found critical times, Eq. (22), and the second order perturbation approximations, from Eq. (43). As expected, the second order approximation captures the behaviour of both layer configurations with more accuracy than the first order approximation, giving accurate results for as few as two repeated layers. It also captures the local maximum in the 'Num. [0.1,1]' solution. Analytically this maximum can be found by differentiating Eq. (43) with respect to n, noting $l = L/n$, to give

$$\frac{dt_c}{dn} \approx \frac{-t_c^{(1)}L}{n^2} - \frac{2t_c^{(2)}L^2}{n^3}. \tag{50}$$

Setting this to zero and solving to find when n is at its maximum gives

$$n_{\max} \approx \frac{-2t_c^{(2)}L}{t_c^{(1)}}. \tag{51}$$

For example if $\alpha = 0.8435$, $\theta_1 = 1$ and $\theta_2 = 0$,

$$n_{\max} \approx \frac{1}{36}\left(1 - \frac{D_{\text{av}}}{D_A}\right)(\pi^4 + 3\pi^2 + 36). \tag{52}$$

This has a negative, non-physical solution for $D_{\text{av}} > D_A$, hence the maximum only occurs for one of the cases explored above.

For the same values used to generate the above figures, $n_{\max} \approx 3.7$. Since it is not possible to have a fraction of layer, this becomes $n_{\max} \approx 4$, which is two repeated layers. This corresponds

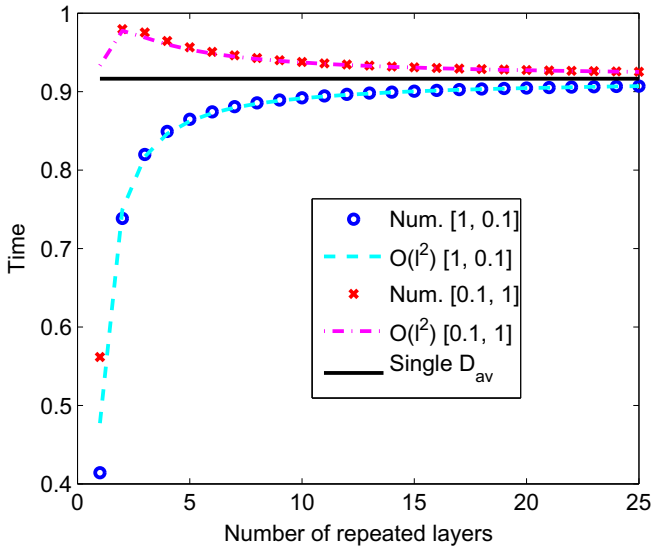

Fig. 4. Numerical solutions for the exact, Eq. (22), and second order perturbed, from Eq. (43), multilayer critical times. The same parameters are used as in Fig. 3.

to the result obtained in Fig. 4. The plot of the third order provides no new insight, as it does not detect the sharp drop. Calculation of the fourth order is restricted by complexity and computational power.

Hence for this example it takes longer for a four layer medium to heat up than any other number of layers. However, it is unclear physically why this should be the case. A deeper understanding of why this maximum occurs, particularly in other geometries and layer configurations (for example a triperiodic region) is the subject of further research.

6. Discussion

The perturbed multilayer critical time, Eq. (43), appears complicated due to its generality. Hence, we discuss solutions with a specific simplified set of values. We assume a biperiodic region with $\theta_1 = 1,\ \theta_2 = 0,\ f_i = 0$, and $\alpha = 0.8435$. Therefore Eq. (43) becomes

$$t_c = \frac{L^2}{6D_{\text{av}}} - \left(1 - \frac{D_{\text{av}}}{D_A}\right)\frac{Ll}{\pi^2 D_{\text{av}}} + O(l^2). \tag{53}$$

Alternatively, the critical time can written as $t_c = L^2/(6D_{\text{eff}})$, giving

$$D_{\text{eff}} = D_{\text{av}} + \frac{6}{\pi^2}\left(1 - \frac{D_{\text{av}}}{D_A}\right)\frac{D_{\text{av}} l}{L} + O(l^2). \tag{54}$$

In both Eqs. (53) and (54) the key term is $(1 - D_{\text{av}}/D_A)$. Using Eq. (25),

$$\left(1 - \frac{D_{\text{av}}}{D_A}\right) = \left(1 - \frac{2}{1 + \frac{D_A}{D_B}}\right). \tag{55}$$

If $D_A = D_B$ then $(1 - D_{\text{av}}/D_A) = 0$, naturally giving the single layer solution. If $D_A > D_B$ then $(1 - D_{\text{av}}/D_A) > 0$ while if $D_A < D_B$, $(1 - D_{\text{av}}/D_A) < 0$. This gives the symmetric behaviour of the critical time for the [0.1,1] and [1,0.1] cases illustrated.

The alternate critical time definition, Eq. (5), determines when the flux at one of the boundaries approaches steady state flow, whereas the definition we have explored, Eq. (7), finds when the average temperature of the medium reaches a chosen proportion of the average steady state temperature. We reproduced the asymptotic analysis from Crank [15] using the multilayer solution, Eq. (12), giving

$$t_{\text{new}} = -\frac{d_1 L C_m}{\lambda_m \theta_2 D_{\text{av}}}. \tag{56}$$

Using the approximate expressions for C_m from Eq. (41) and λ_m from Eq. (37), gives

$$t_{\text{new}} = t_{\text{new}}^{(0)} + t_{\text{new}}^{(1)} l + t_{\text{new}}^{(2)} l^2 + O(l^3), \tag{57}$$

where $t_{\text{new}}^{(0)}$ is given by Eq. (5), $t_{\text{new}}^{(1)} = 0$, and the second order is given by a complicated hypergeometric function. Further exploration of this critical time definition, along with comparisons with other applicable definitions, are the subject of future work.

While we have only considered biperiodic materials $[A, B]$, with simple boundary and interface conditions, it is possible to extend this work to more complicated situations. We are currently researching other approximate solutions for triperiodic layers $[A, B, C]$, that is $(ABC)(ABC)\ldots$; cases where $l_A \neq l_B$; for mixed boundary and jump interface conditions; using alternative critical time definitions; and for cylindrical and spherical coordinates. Whilst these extensions are possible using the techniques we have demonstrated here, they are nontrivial to find, with great care needed in manipulating the intricate equations, even with the use of symbolic manipulation software. Indeed, even subtle extensions reach current computational limits. Evolution of more efficient computational algebra systems, algorithmic methods for coding these systems, and increased computational power would facilitate further research in this area.

7. Conclusions

Diffusive transport through a multilayered material is nontrivial. In particular, averaging the properties of a multilayered medium does not capture its critical time behaviour, such as the time to reach a specified temperature. By finding the exact solution for multilayer diffusion, and using a perturbation series, we have determined simple expressions which give the critical diffusion time. This corrects the commonly used series-averaged diffusivity method for finding critical times. Importantly it captures the asymmetric behaviour of a multilayered medium; it does matter in which order a material is layered when considering diffusion.

Appendix A. Eigenfunction coefficients

To find the perturbation of Eq. (15), the coefficients $J_{i,m}$ and $K_{i,m}$, Eqs. (16) and (17), must first be analysed. This analysis uses a biperiodic region, where the layers are ordered '*ABABAB*...'. To facilitate this, the coefficients are first written in matrix form. That is, let

$$\mathbf{K}_i = \begin{bmatrix} J_{i,m} \\ K_{i,m} \end{bmatrix}. \tag{58}$$

The recursive relationships established in Eqs. (16) and (17) are then

$$\mathbf{K}_{i+1} = \mathbf{M}_i \mathbf{K}_i,$$

where

$$\mathbf{M}_i = \begin{bmatrix} \frac{d_i}{d_{i+1}} \cos\left(\lambda_m \frac{l}{d_i}\right) & -\frac{d_i}{d_{i+1}} \sin\left(\lambda_m \frac{l}{d_i}\right) \\ \sin\left(\lambda_m \frac{l}{d_i}\right) & \cos\left(\lambda_m \frac{l}{d_i}\right) \end{bmatrix} \tag{59}$$

and

$$\mathbf{K}_1 = \begin{bmatrix} 1 \\ 0 \end{bmatrix}. \tag{60}$$

This matrix notation then allows us to express $\mathbf{K}_i$ as

$$\mathbf{K}_{i_A} = (\mathbf{M}_B\mathbf{M}_A)^{(i-1)/2}\mathbf{K}_1,$$
$$\mathbf{K}_{i_B} = \mathbf{M}_A(\mathbf{M}_B\mathbf{M}_A)^{(i-2)/2}\mathbf{K}_1, \tag{61}$$

where i_A denotes 'A' layers and i_B denotes 'B' layers,

$$\mathbf{M}_A = \begin{bmatrix} \frac{d_A}{d_B}\cos\left(\lambda_m\frac{l}{d_A}\right) & -\frac{d_A}{d_B}\sin\left(\lambda_m\frac{l}{d_A}\right) \\ \sin\left(\lambda_m\frac{l}{d_A}\right) & \cos\left(\lambda_m\frac{l}{d_A}\right) \end{bmatrix} \quad \text{and}$$
$$\mathbf{M}_B = \begin{bmatrix} \frac{d_B}{d_A}\cos\left(\lambda_m\frac{l}{d_B}\right) & -\frac{d_B}{d_A}\sin\left(\lambda_m\frac{l}{d_B}\right) \\ \sin\left(\lambda_m\frac{l}{d_B}\right) & \cos\left(\lambda_m\frac{l}{d_B}\right) \end{bmatrix}.$$

$\mathbf{M}_{BA} = \mathbf{M}_B\mathbf{M}_A$ is then diagonalised. That is, for 'A' layers,

$$\mathbf{M}_{BA}^{(i-1)/2} = \mathbf{P}\mathbf{D}^{(i-1)/2}\mathbf{P}^{-1} = \mathbf{P}\begin{bmatrix}\omega_1 & 0\\ 0 & \omega_2\end{bmatrix}^{(i-1)/2}\mathbf{P}^{-1}$$
$$= \mathbf{P}\begin{bmatrix}\omega_1^{(i-1)/2} & 0\\ 0 & \omega_2^{(i-1)/2}\end{bmatrix}\mathbf{P}^{-1}, \tag{62}$$

where $\mathbf{D}$ is a diagonal matrix with elements the eigenvalues, ω_1 and ω_2, of $\mathbf{M}_{BA}$, and $\mathbf{P}$ contains the corresponding eigenvectors. Therefore Eq. (61) becomes

$$\mathbf{K}_{i_A} = (\mathbf{P}\mathbf{D}^{(i-1)/2}\mathbf{P}^{-1})\mathbf{K}_1,$$
$$\mathbf{K}_{i_B} = \mathbf{M}_A(\mathbf{P}\mathbf{D}^{(i-2)/2}\mathbf{P}^{-1})\mathbf{K}_1. \tag{63}$$

The matrix $\mathbf{M}_{BA}$ is not shown due to its considerable size, however its eigenvalues, ω_1 and ω_2, are given by the two solutions of

$$\omega^2 + 2\omega\left[\left(\frac{d_A}{d_B}+\frac{d_B}{d_A}\right)\sin\left(\lambda_m\frac{l}{d_A}\right)\sin\left(\lambda_m\frac{l}{d_B}\right) - \cos\left(\lambda_m\frac{l}{d_A}\right)\right.$$
$$\left.\times\cos\left(\lambda_m\frac{l}{d_B}\right)\right] + 1 = 0. \tag{64}$$

The next step is to evaluate the eigenvalues to the relevant powers, such as $\omega_1^{(i-1)/2}$ in Eq. (63). First, the index i is written in terms of l as $i = (1 + x_{i-1}/l)$, such that $(i-1)/2 = x_{i-1}/(2l)$ and $i/2 - 1 = (x_{i-1} - l)/(2l)$ for the A and B layers, respectively. Second, a perturbation series of the resulting expressions are calculated. Finally, d_B is rewritten in terms of d_{av}, and the expressions are simplified:

$$\omega_{i_A}^{(i-1)/2} = \omega_{i_A}^{x_{i-1}/2l} \to \exp\left(\pm\frac{Ix_{i-1}\lambda_m}{d_{\text{av}}}\right) + O(l^2), \tag{65}$$

$$\omega_{i_B}^{(i-2)/2} = \omega_{i_B}^{(x_{i-1}-l)/2l} \to \exp\left(\pm\frac{Ix_{i-1}\lambda_m}{d_{\text{av}}}\right)\left[1 \mp \frac{I\lambda_m}{d_{\text{av}}}l + O(l^2)\right], \tag{66}$$

where $I = \sqrt{-1}$ and the exponential forms were expected from the relationship between the eigenvalue expressions and the powers with l. The two eigenvalues, ω_1 and ω_2, are contained within Eqs. (65) and (66) as the $\pm/\mp$ solutions. The eigenvectors, $\mathbf{V}_j$, which form the columns for $\mathbf{P}$ are

$$\mathbf{V}_j = \begin{bmatrix}\mathbf{M}_{BA}[2,2] - \omega_j \\ -\mathbf{M}_{BA}[2,1]\end{bmatrix}, \quad j = 1,2 \tag{67}$$

where, for example, [2,1] denotes the second row and first column of $\mathbf{M}_{BA}$.

Substituting Eqs. (65) and (67) into Eq. (63) for the 'A' layers gives,

$$J_{i_A,m} = \cos\left(\frac{\lambda_m x_{i-1}}{d_{\text{av}}}\right) + \frac{\lambda_m(D_A - D_{\text{av}})}{2d_{\text{av}}D_A}\sin\left(\frac{\lambda_m x_{i-1}}{d_{\text{av}}}\right)l + O(l^2)$$
$$K_{i_A,m} = \frac{d_A}{d_{\text{av}}}\sin\left(\frac{\lambda_m x_{i-1}}{d_{\text{av}}}\right) + O(l^2), \tag{68}$$

denoted by i_A. Similarly, for the 'B' layers,

$$J_{i_B,m} = \frac{\sqrt{2D_A - D_{\text{av}}}}{d_{\text{av}}}\left[\cos\left(\frac{\lambda_m x_{i-1}}{d_{\text{av}}}\right) + \frac{\lambda_m(D_A - D_{\text{av}})}{2D_A d_{\text{av}}}\sin\left(\frac{\lambda_m x_{i-1}}{d_{\text{av}}}\right)l\right] + O(l^2)$$
$$K_{i_B,m} = \frac{d_A}{d_{\text{av}}}\sin\left(\frac{\lambda_m x_{i-1}}{d_{\text{av}}}\right) - \frac{\lambda_m(D_A - D_{\text{av}})}{d_A D_{\text{av}}}\cos\left(\frac{\lambda_m x_{i-1}}{d_{\text{av}}}\right)l + O(l^2). \tag{69}$$

Appendix B. Solution perturbation series

Each term in Eq. (42) is shown in full. The zeroth and first order 'A' layer terms, respectively, are

$$U_A^{(0)}(x,t) = \theta_1 + \frac{(\theta_2-\theta_1)x}{L} - \left(1 - \frac{D_{\text{av}}}{D_A}\right)\frac{(\theta_2-\theta_1)(x - x_{i-1})}{L}$$
$$+ \sum_{m=1}^{\infty} e^{-\lambda_m^2 t}\frac{((-1)^m\theta_2 - \theta_1)}{m\pi}\left\{\left(1 + \frac{d_{\text{av}}}{d_A}\right)\sin(\omega_m[x_A + x_{i-1}])\right.$$
$$\left. - \left(1 - \frac{d_{\text{av}}}{d_A}\right)\sin(\omega_m[x_A - x_{i-1}])\right\}, \tag{70}$$

$$U_A^{(1)}(x,t) = \left(1 - \frac{D_{\text{av}}}{D_A}\right)\frac{\omega_m d_{\text{av}}}{2d_A}\sum_{m=1}^{\infty} e^{-\lambda_m^2 t}\frac{((-1)^m\theta_2 - \theta_1)}{m\pi}$$
$$\times\{\cos(\omega_m[x_A - x_{i-1}]) - \cos(\omega_m[x_A + x_{i-1}])\}, \tag{71}$$

with

$$x_A = \frac{(x - x_{i-1})d_{\text{av}}}{d_A}, \quad \omega_m = \frac{m\pi}{L}. \tag{72}$$

The zeroth and first order 'B' layer terms are

$$U_B^{(0)}(x,t) = \theta_1 + \frac{(\theta_2-\theta_1)}{L}\left(\frac{d^\star}{d_A}x_B + x_{i-1}\right) + \sum_{m=1}^{\infty} e^{-\lambda_m^2 t}\frac{((-1)^m\theta_2 - \theta_1)}{m\pi}$$
$$\times\left\{\left(1 + \frac{d^\star}{d_A}\right)\sin(\omega_m[x_B + x_{i-1}]) - \left(1 - \frac{d^\star}{d_A}\right)\sin(\omega_m[x_B - x_{i-1}])\right\}, \tag{73}$$

$$U_B^{(1)}(x,t) = -\left(1 - \frac{D_{\text{av}}}{D_A}\right)\frac{(\theta_2-\theta_1)}{L} + \frac{1}{2L}\left(1 + \frac{d^\star}{d_A}\right)\left(1 - \frac{d^\star}{d_A}\right)$$
$$\times\sum_{m=1}^{\infty} e^{-\lambda_m^2 t}((-1)^m\theta_2 - \theta_1)\left\{\left(2 + \frac{d^\star}{d_A}\right)\cos(\omega_m[x_B + x_{i-1}])\right.$$
$$\left. + \left(2 - \frac{d^\star}{d_A}\right)\cos(\omega_m[x_B - x_{i-1}])\right\}, \tag{74}$$

with

$$x_B = \frac{d^\star(x - x_{i-1})}{d_A}, \quad d^\star = \sqrt{2D_A - D_{\text{av}}}. \tag{75}$$

The $(1 - D_{\text{av}}/D_A)$ term is of particular interest as it allows the solution to be either side of the averaged single layer.

Appendix C. Alternative critical time

Previous authors [11–13], derived an expression for the critical time in layered materials as

$$t = \left[\sum_{i=1}^{n}\frac{l_i}{d_i^2}\right]^{-1}\left[\sum_{i=1}^{n}\left\{\frac{l_i^2}{2d_i^2}\sum_{j=i}^{n}\left(\frac{l_j}{d_j^2}\right) - \frac{l_i^3}{3d_i^4}\right\}\right.$$
$$\left. + \sum_{i=1}^{n-1}\left\{\frac{l_i}{d_i^2}\sum_{k=i+1}^{n}\left(l_k\sum_{j=k}^{n}\left[\frac{l_j}{d_j^2}\right] - \frac{l_k^2}{2d_k^2}\right)\right\}\right]. \tag{76}$$

Their method integrated Eq. (1) from x to x_i with respect to x, then integrated again from $x = x_{i-1}$ to x_i and summed the result from $i = 1 \ldots n$. Eq. (1) was then integrated from $x = x_{i-1}$ to x_i and summed from $i + 1$ to n, and substituted into the previous expres-

sion. This resulted in an expression for the flux across the outgoing surface, $x = x_n$, which was then integrated from $t = 0$ to t to calculate the total mass. The asymptote of the total mass was then found as $t \to \infty$.

This result is illustrated in Fig. 3 but does not accurately reflect the critical time we have found, nor does it identify the asymmetric nature of the critical time.

References

[1] S.I. Barry, W.L. Sweatman, Modelling heat transfer in steel coils, ANZIAM J. (E) 50 (2009) C668.

[2] M. McGuinness, W.L. Sweatman, D.Y. Baowan, S.I. Barry, Annealing steel coils, in: T. Marchant, M. Edwards, G.N. Mercer (Ed.), MISG 2008 Proceedings, 2009.

[3] W.Y.D. Yuen, Transient temperature distribution in a multilayer medium subject to radiative surface cooling, Appl. Math. Model. 18 (1994) 93–100.

[4] G. Pontrelli, F. de Monte, Mass diffusion through two-layer porous media: an application to the drug-eluting stent, Int. J. Heat Mass Transfer 50 (2007) 3658–3669.

[5] K. Landman, M. McGuinness, Mean action time for diffusive processes, J. Appl. Math. Decis. Sci. 4 (2) (2000) 125–141.

[6] A. McNabb, G.C. Wake, Heat conduction and finite measures for transition times between steady states, IMA J. Appl. Math. 47 (2) (1991) 192–206.

[7] A. McNabb, Mean action times, time lags and mean first passage times for some diffusion problems, Math. Comput. Model. 18 (10) (1993) 123–129.

[8] R.I. Hickson, S.I. Barry, G.N. Mercer, Critical times in multilayer diffusion. Part 1: Exact solutions, Int. J. Heat Mass Transfer (accepted) (2009).

[9] R.I. Hickson, S.I. Barry, G.N. Mercer, Exact and numerical solutions for effective diffusivity and time lag through multiple layers, ANZIAM J. (E) 50 (2009) C682–C695.

[10] M.F.A. Azeez, A.F. Vakakis, Axisymmetric transient solutions of the heat diffusion problem in layered composite media, Int. J. Heat Mass Transfer 43 (2000) 3883–3895.

[11] R. Ash, R.M. Barrer, D.G. Palmer, Diffusion in multiple laminates, Brit. J. Appl. Phys. 16 (1965) 873–884.

[12] R. Ash, R.M. Barrer, J.H. Petropoulos, Diffusion in heterogeneous media: properties of a laminated slab, Brit. J. Appl. Phys. 14 (1963) 854–862.

[13] R.M. Barrer, Diffusion and permeation in heterogenous media, in: J. Crank, G.S. Park (Eds.), Diffusion in Polymers, Academic Press, London, 1968, pp. 165–215.

[14] Maple, Maplesoft, Waterloo, Ontario. Available from: <http://www.maplesoft.com/>.

[15] J. Crank, The mathematics of diffusion, Oxford University press, England, 1957.